AGU PUBLICATIONS

Tectonics

RESEARCH ARTICLE
10.1002/2013TC003406

Key Points:
- We revealed the pristine structure of Adria margin accreted in the Apennines
- The pristine structure of Adria conditioned the evolution of the belt
- We document the inversion of normal faults

Correspondence to:
C. Chiarabba,
claudio.chiarabba@ingv.it

Citation:
Chiarabba, C., P. De Gori, D. Latorre, and A. Amato (2014), Crustal structure in the area of the 2002 Molise earthquake: Clues for the evolution of the southern Apennines, *Tectonics*, *33*, doi:10.1002/2013TC003406.

Received 3 JUL 2013
Accepted 24 MAR 2014
Accepted article online 27 MAR 2014

Crustal structure in the area of the 2002 Molise earthquake: Clues for the evolution of the southern Apennines

C. Chiarabba[1], P. De Gori[1], D. Latorre[1], and A. Amato[1]

[1]Istituto Nazionale di Geofisica and Vulcanologia, CNT, Rome, Italy

Abstract The Apennines is a mountain belt with paired extension and compression that are explained by the subduction and delamination of the Ionian/Adria lithosphere. During the belt formation, the Adria crust is flexed downward and then incorporated into the wedge after peeling off along some weak level whose origin is still discussed. In southern Apennines, this process seems to have stopped at about 0.7 Ma by the development of a tear in the subducting lithosphere and consequent extension that spread along the mountain range. Seismological data acquired after the 2002 *Mw* 6.0 Molise strike-slip earthquake yield modeling the structure of the Adria crust as congealed close to the leading edge of the belt. Tomography images show inverted normal faults within the sedimentary cover (Apulian units). Fault inversion, incomplete close to the compressional front, testifies for a final squeezing of the entire, previously flexed, Apulian continental margin. Pronounced high *Vp* and low *Vp/Vs* anomalies are observed at depth greater than 12 km and undoubtfully attributed to heterogeneities of the basement, solving the long-lasting contention on the nature of similar high-speed bodies observed beneath the Apennines. Beneath these bodies, we observe a strong reflectivity, suggesting the presence of a fluid-filled layer in the middle lower crust that may act as a decoupling level in the Apennines tectonics. The deep fluids are also favoring the rupture of strike-slip earthquakes, like those that occurred in 2002, and the intermediate-depth seismicity diffused in the Apulian region.

1. Introduction

The Apennines formed after the subduction of the Tethys Ocean in the Cenozoic, for the collision between Africa and Europe, part of a broad mountain system that heals the two plates from Gibraltar to Turkey [*Dercourt et al.*, 1986; *Dewey et al.*, 1989; *Jolivet and Faccenna*, 2000]. Since about 35 Ma, the collision involved the continental margins of the Tethys Ocean that are complex in structure. In fact, during the margin formation, shear zones develop within continents [*Lister et al.*, 1986; *Jolivet et al.*, 2009, and references therein]. These preexisting weak zones, which developed along the margin, are potentially able to control the subsequent deformation, for instance, once the margin is inverted by compression [*Butler et al.*, 2006; *Tavani et al.*, 2013]. In addition, extensional faulting and fracturing were also associated with bending of the Adria lithosphere during forebulge and foredeep stages that produced normal faults during Miocene [e.g., *Vitale et al.*, 2012].

Although less tectonically active than the adjacent eastern Mediterranean regions, the southern Apennines offer a good opportunity to investigate how the margin complexity affects the collision because of the abundant geologic and geophysical data summarized in a vast literature (*Royden et al.* [1987], *Doglioni et al.* [1996], and *Mazzoli et al.* [2008], among an avenue of many others).

Collisional models for the Apennines invoke that the crust is delaminated. In thin- or thick-skinned tectonic models [*Bally et al.*, 1986; *Roure et al.*, 1991; *Tozer et al.*, 2002; *Butler et al.*, 2004; *Scrocca et al.*, 2005], such décollement is placed along the Triassic evaporites or deeper in the crust, respectively. The poor illumination of the deep crust in the Apennines belt by commercial seismic profiles does not enable to discriminate between the two alternative models. *Steckler et al.* [2008] use receiver function analysis to suggest that a thick-skin style is more suited to southern Apennines, as also suggested by magnetic modeling [*Speranza and Chiappini*, 2002].

The uncertainty in the tectonic style led to estimate a rather different amount of shortening that ranges between some tens to a few hundred kilometers. The latter implies a very shallow décollement and the subduction of a relevant portion of the continental lithosphere still unseen by mantle tomography [*Lucente et al.*, 1999; *Piromallo and Morelli*, 2003; *Giacomuzzi et al.*, 2010].

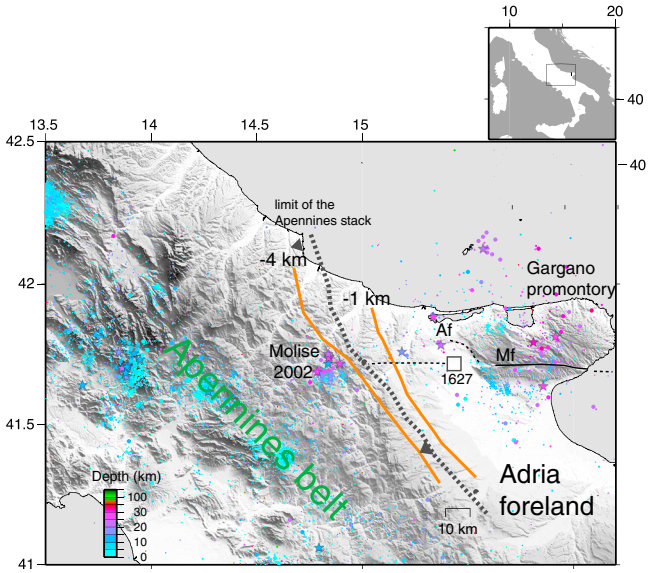

Figure 1. Map of the investigated region of southern Apennines. Colored dots represent hypocenters of past years seismicity. Dashed line is the limit of the Apennines stack at depth. Orange lines indicate the depth of the Apulian carbonate platform westward dipping below the Apennines belt, simplified from *Nicolai and Gambini* [2007]. The 2002 seismicity occurs mostly at the edge, and at midcrustal depths, of the Apennines orogen. Mf is the Mattinata fault, Af the Apricena fault, see *Patacca and Scandone* [2004]. The approximate epicenter of the 1627 A.D., *M* 6.7 earthquake is shown.

Structural studies focused on the Mesozoic rootless nappes [*Mostardini and Merlini*, 1986; *Patacca and Scandone*, 1989; *Menardi Noguera and Rea*, 2000; *Mazzoli et al.*, 2006] and the uppermost part of the Apulian platform, locus of oil reservoirs [*Shiner et al.*, 2004]. The only deep crustal survey carried out in the southern Apennines (CROP04) [*Patacca and Scandone*, 2007] is elusive in providing constraints for the structure at great depths. On the contrary, passive seismic tomographic studies [*Bisio et al.*, 2004; *Chiarabba and Amato*, 1997; *Chiarabba et al.*, 2010; *Valoroso et al.*, 2011] reported the existence of ultraspeed bodies in the middle crust of the Apennines interpreted as basement rocks involved in the thrusts, but duplex structures of dolomites units (that have very high *P* wave velocities) cannot be excluded. At greater depths, *P* and *S* wave velocity inversions are revealed in the middle lower crust [*Chiarabba et al.*, 2009; *Di Stefano et al.*, 2009]. Positive magnetic anomalies are found to the east of the belt, suggesting that high susceptibility rocks are present underneath the poorly magnetic Mesozoic cover at depths below 15–20 km, depending on the assumed geothermal gradient [*Speranza and Chiappini*, 2002].

In this study, we use seismologic data collected during the Molise 2002 earthquake sequence to define the nature and structure of the Adria crust in a region and in a volume poorly sampled until now. Its key position, close to the leading edge of the Apennines front (see Figure 1), is perfect to address the pristine structure of the Adria lithosphere, still not significantly involved in the compressional tectonics. The unusual depth of the earthquake sequence (6–18 km depth [*Chiarabba et al.*, 2005]) yields computation of velocity models down to the depth of the pre-Mesozoic basement with a resolution never attained so far by active and passive seismology and offering solution of the long-lasting debate on the nature of the high-velocity bodies.

2. Data and Tomographic Inversion

After the 2002 *Mw* 6.0 Molise earthquake, a dense portable seismic network consisting of 37 seismic stations was installed to record aftershocks. A total of 1929 events was located by *Chiarabba et al.* [2005] and shows the about 20 km long E-W trending strike-slip fault that failed with two main dextral strike-slip ruptures [*Di Bucci and Mazzoli*, 2003; *Di Luccio et al.*, 2005].

From the entire catalog of aftershocks, we selected earthquakes that have starting hypocentral errors less than 1 km (in *x*, *y*, and *z*), azimuthal gap less than 180°, and an average number of *P* and *S* wave arrivals equal to 16 and 10, respectively (Figure 2). Data are those read on digital waveforms and already used by *Chiarabba et al.* [2005] to locate the earthquakes. Reading accuracy of arrival times read on digital waveforms is on the order of 0.02–0.10 s and weighted according to the following scheme [*Chiarabba et al.*, 2005]: weight 100% for reading errors less than 0.02 s, 75% for errors between 0.02 and 0.05 s, 50% for errors between 0.05 and 0.1, and 25% for errors higher than 0.1 s.

We use the Simulps14q inversion code [*Haslinger*, 1998] to invert for velocity and hypocentral parameters, optimizing the solution with damping parameters that balance the data misfit reduction and model complexity. The coupling between hypocentral and velocity parameters is resolved by the

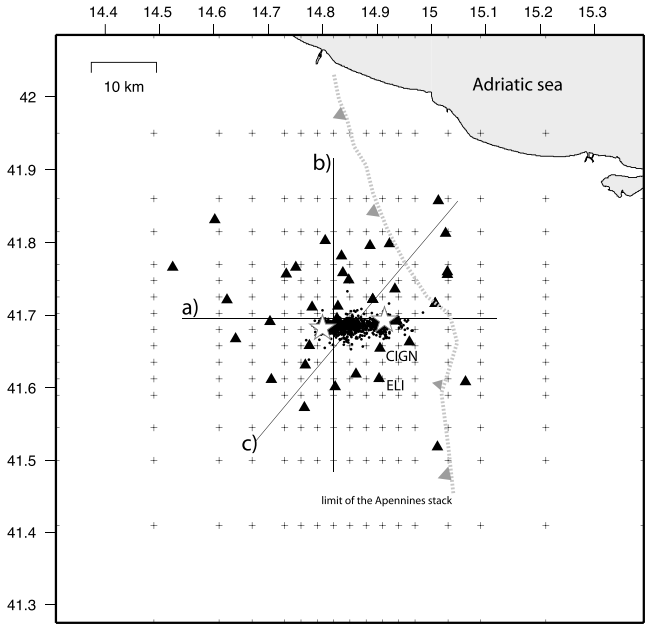

Figure 2. Data used in the tomographic inversion: Triangles are the temporary seismic stations, black dots are the used earthquakes, and the crosses are the inverted nodes. The white stars indicate the two main shocks of the 2002 sequence. The traces of sections plotted in Figure 5 are also shown.

parameter separation as long as the starting values are close to the real ones. The model is parameterized by a 3-D grid of nodes with velocity continuously varying through the medium and seismic rays are traced using the approximate ray tracing (ART) pseudo-bending method [*Thurber*, 1983; *Um and Thurber*, 1987].

Due to the geometry of earthquakes and receivers, the mostly vertical upcoming rays yield a significant smearing of anomalies in the uppermost crust layers. We decided to help the inversion by assigning an a priori geometry for the top of the Apulian carbonate platform that is well constrained by both seismic survey profiles [*Nicolai and Gambini*, 2007; *Mariotti and Doglioni*, 2000] and analysis of converted phases [*Latorre et al.*, 2010]. *Vp* values typical of limestone rocks are assigned to nodes below this depth. After trying different grid sizes, the best balance between model resolution and fidelity is achieved with nodes placed at a distance of 3 km (in *x* and *y*) and layers every 2 depth. The starting uniform *Vp*/*Vs* value of 1.8 is taken from *Chiarabba et al.* [2005]. Although the geometry of the Apulia top is assigned a priori, the velocities in the uppermost layer can be modified during the tomographic inversion.

We use a total of 21,594 *P* wave arrival times and 14,441 *S-P* times from 1332 earthquakes recorded at 37 seismic stations to invert for 1516 and 5328 velocity and hypocentral parameters, respectively. After four iteration steps, we obtain a variance reduction equal to 57% and a final total root-mean-square of 0.14 s. The final data variance is quite the double for *S-P* than for *P* wave arrival times. Formal hypocentral errors in the 3-D model are less than 0.5 km in *x*, *y*, and *z* on average.

2.1. Model Resolution

The reliability of the velocity models has been assessed by a complete analysis of the Resolution Matrix [*Menke*, 1989]. A measure of model reliability is given by the sharpness of each row in the resolution matrix, quantified in a very compact form by the spread function (SF). Following the literature, the entire resolution matrix is analyzed and the spread of the matrix is computed to establish the threshold value that encompasses delta-like vectors [see *Toomey and Foulger*, 1989; *Michelini and McEvilly*, 1991].

In our case, a value of spread function smaller than 1.7 indicates that the model parameter is adequately well resolved. The averaging of velocity estimation is indeed centered on the model parameter, without a significant, undesired contribution from those of adjacent nodes (i.e., without lateral or vertical smearing of anomalies). Figure 3a shows that the resolution is good for central nodes in layers located between 6 and 14 km depth, while the shallower layer (at 4 km depth) has a more pronounced vertical smearing of anomalies. In the entire central region, more than 70% of each resolution matrix row is centered on the right parameter. The amount of lateral and vertical smearing varies from very negligible (Figure 3b, node c) to small (node b) and sensible (in the vertical direction, node a), from spread function values lower than 1.0, 1.5, and higher than 1.7, respectively. The vast literature on local earthquake tomography shows that the region indicated as resolved by the spread function analysis always coincides with that resolved by synthetic tests. Only anomalies located within the well-resolved volume, encircled by spread function 1.7 contour line, are discussed and interpreted.

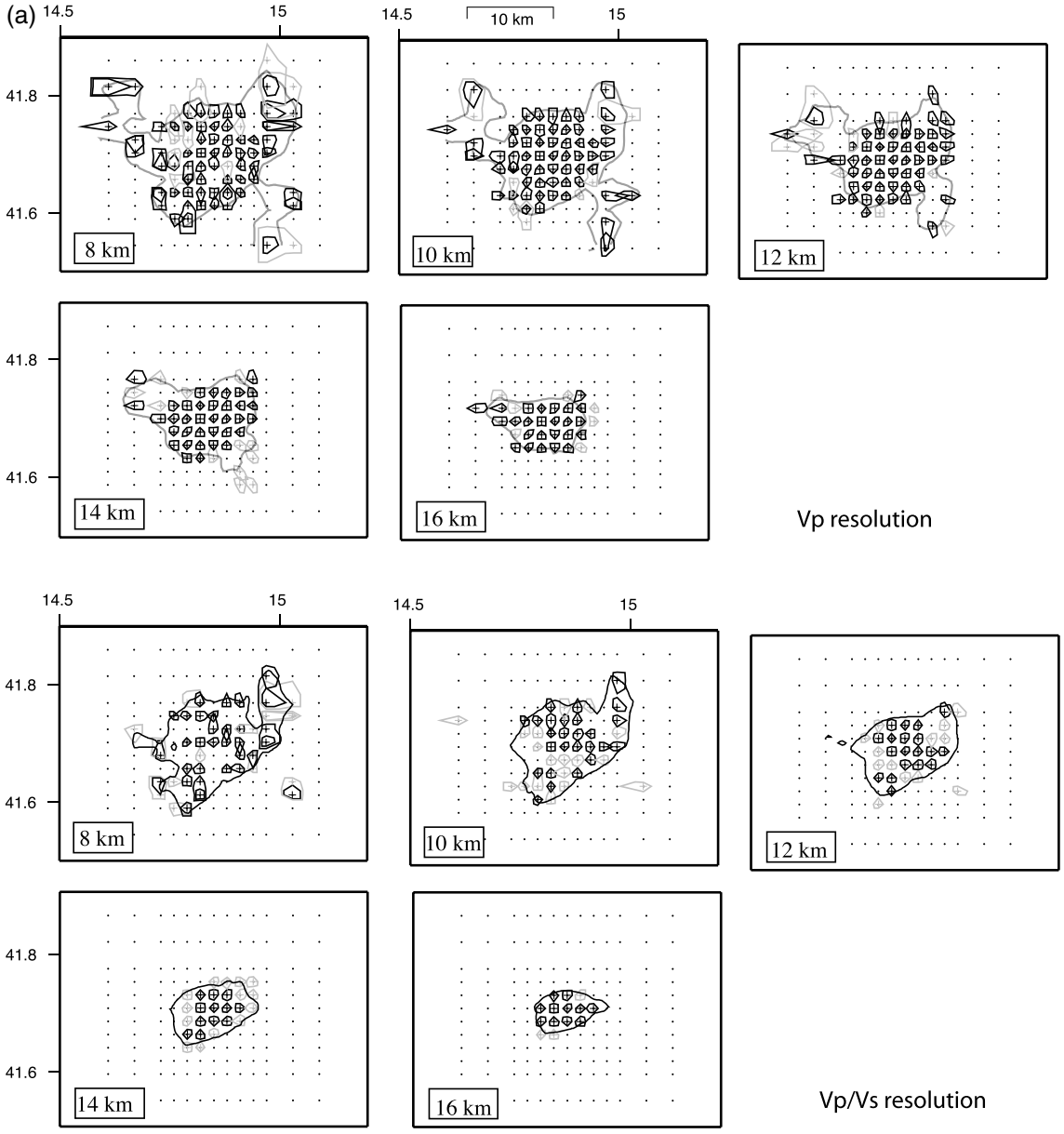

Figure 3. (a) Map of the 70% smearing contouring for inverted nodes (crosses) with spread function (SF) lower or equal to 1.7 in layers from 6 to 14 km depth. The nodes with SF < 1.50 and with 1.50 < SF < 1.70 have black and gray crosses and contours, respectively. Dashed lines encompass the resolved regions of the model, and are the same plotted in Figure 4 on the velocity model. (b) Vertical section parallel to the fault showing the 70% smearing contours for three nodes with high (node a) to low values (node c) of the spread function that show difference in resolution and smearing properties. Node c is a perfectly resolved node.

3. Velocity Model Results

In the layers 8 to 12 km depth (Figure 4 and sections in Figure 5), *P* wave model shows a main low *Vp* anomaly located in the central part of the area, surrounded by positive anomalies (*Vp* between 6.0 and 6.4 km/s). This velocity pattern reflects both the general westward deepening of the Apulian carbonate platform [see *Mariotti and Doglioni*, 2000] and a local up-warping of the carbonate layer due to compressive faults in the Apennines stack, in the western part of the model. The overall geometry of the Adria platform, depressed in the central part of the model, and the 4.9 km/s isovelocity contour well matches with the top of the carbonate units defined by *S-P* converted wave analysis [see *Latorre et al.*, 2010].

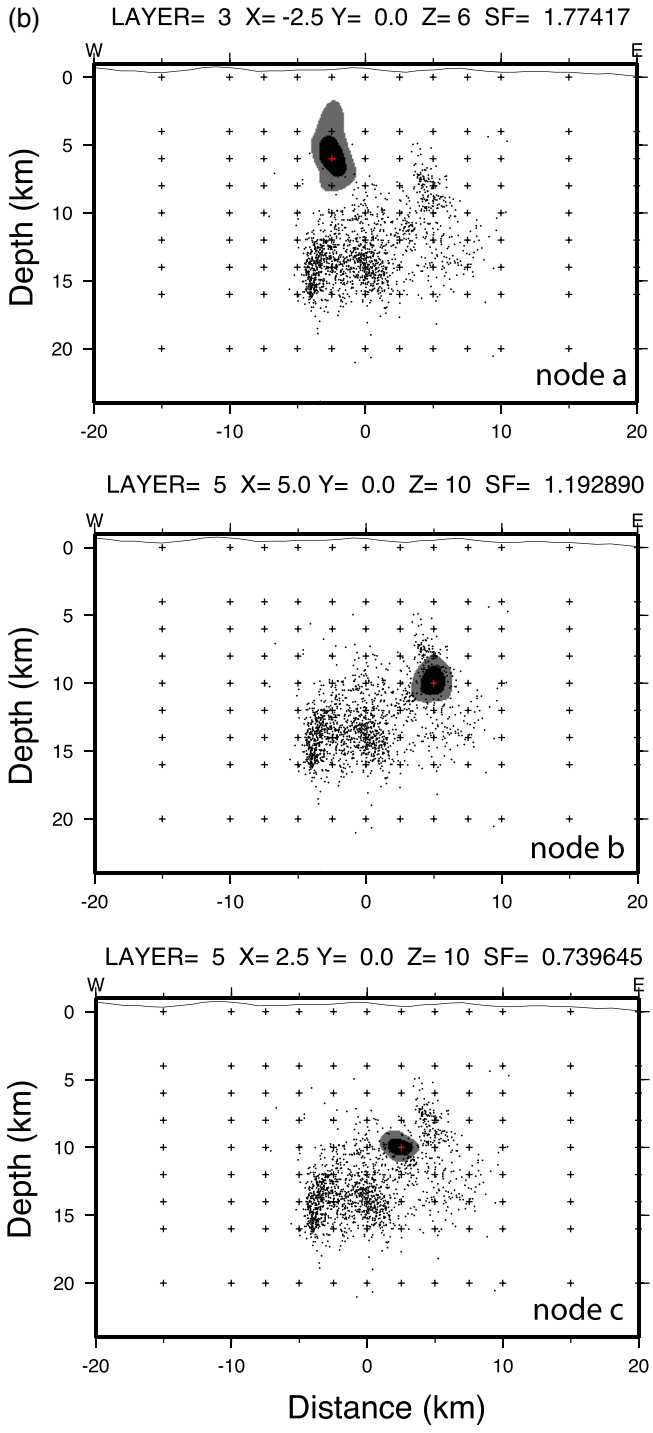

Figure 3. (continued)

At greater depths, very high *Vp* anomalies (*Vp* higher than 6.4 km/s and up to 7.0 km/s) are found in distinct positive spots that cluster close to the fault at depth.

The *Vp*/*Vs* model shows two main features: positive anomalies in the central area along the east trending fault between 8 and 10–12 km and a change from negative to positive anomalies crossing the fault from north to south below 12 km depth.

The first shallow high *Vp*/*Vs* anomaly coincides with relatively low *Vp* anomalies (*Vp* between 5.2 and 6.0 km/s) and suggests that the Adria carbonate layer (always characterized by relatively high *Vp* and high *Vp*/*Vs* in the Apennines [see *Chiarabba and Amato*, 2003]) is down-warped in the central area. The values found in the upper 10 to 12 km of the crust (ranging between 5.8 and 6.4 km/s) are consistent with the presence of the Meso-Cenozoic carbonate rocks [see *Valoroso et al.*, 2011], lying below low-velocity Plio-Pleistocene sediments. The *P* wave velocity within the platform varies between 4.9 and 6.4 km/s, and *Vp* is never faster than 6.5 km/s. The warping of velocity anomalies defines the existence of faults that cut the sedimentary cover (see sections b and c in Figure 5). At greater depth, very high velocity materials are found (*Vp* as high as 7.0 km/s).

The second feature is very interesting. Across the E-W trending fault, sharp velocity contrasts are present at depths larger than 12 km (Figure 4), while in its uppermost part, i.e., within the Mesozoic carbonate layer, this abrupt variation is lost and replaced by a broad low-velocity anomaly. These crustal heterogeneities might indicate that most of the strike-slip activity of the E-W trending fault was related to a tectonic phase older than the Apennines tectonics, while a more recent reactivation of the system led to the development of a dilational jog at a fault bend, as also suggested by *Latorre et al.* [2010].

The overall geometry of the fault system activated in 2002 is enhanced by the distribution of 3-D-located aftershocks (Figure 6). The alignment of earthquakes delineates a 10–15 km long E-W trending subvertical structure, while small portions seem to be slightly north dipping (see sections 3 and 5). Aftershocks tend to cluster between 12 and 16 km depth.

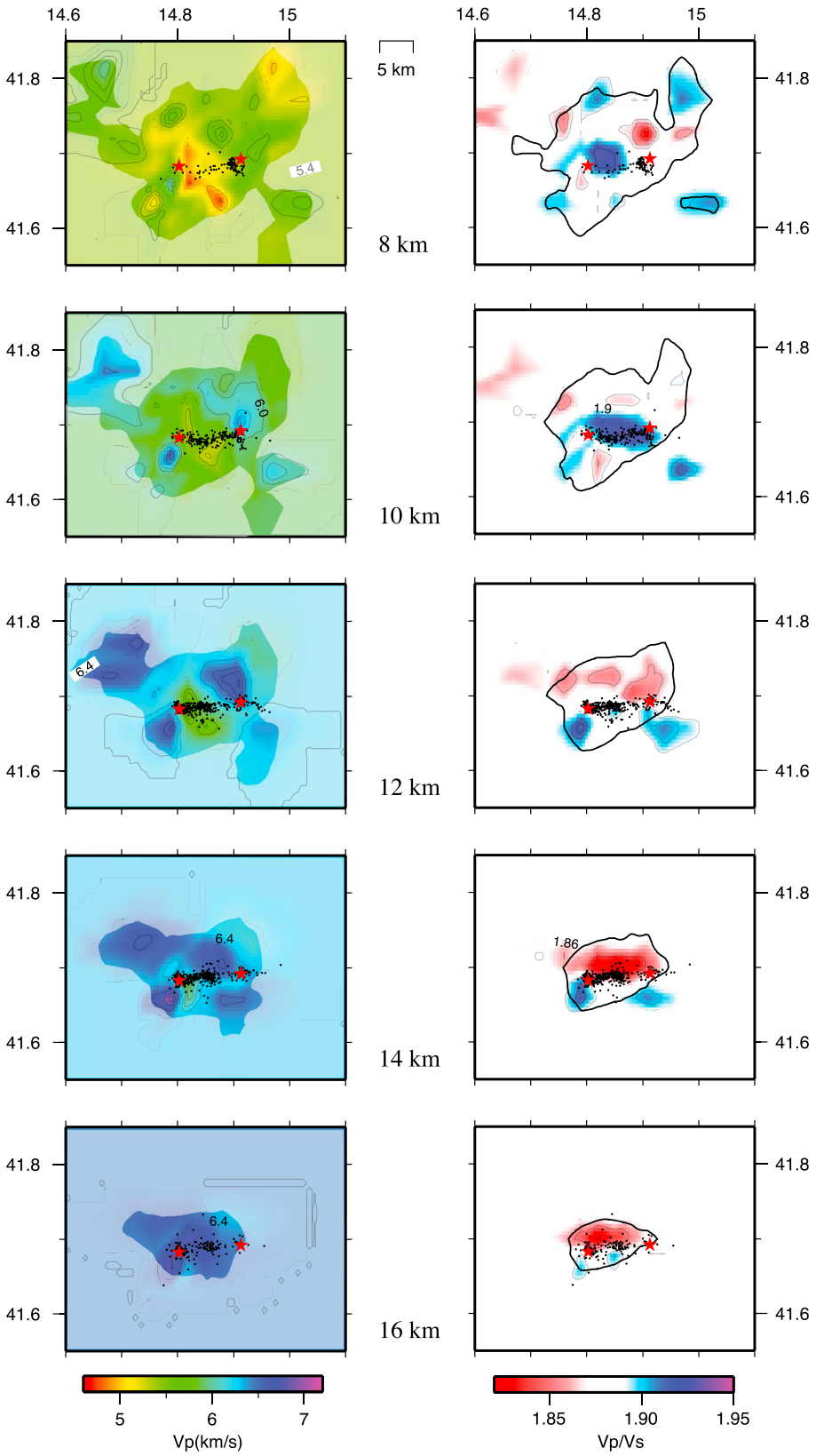

Figure 4. *Vp* and *Vp/Vs* models in the inverted layers. The black lines indicate the SF = 1.7 isoline, encompassing the well-resolved region (see Figure 3). Earthquakes occurring ±1 km from each layer are plotted as black dots. The red stars are the two main shocks hypocenters.

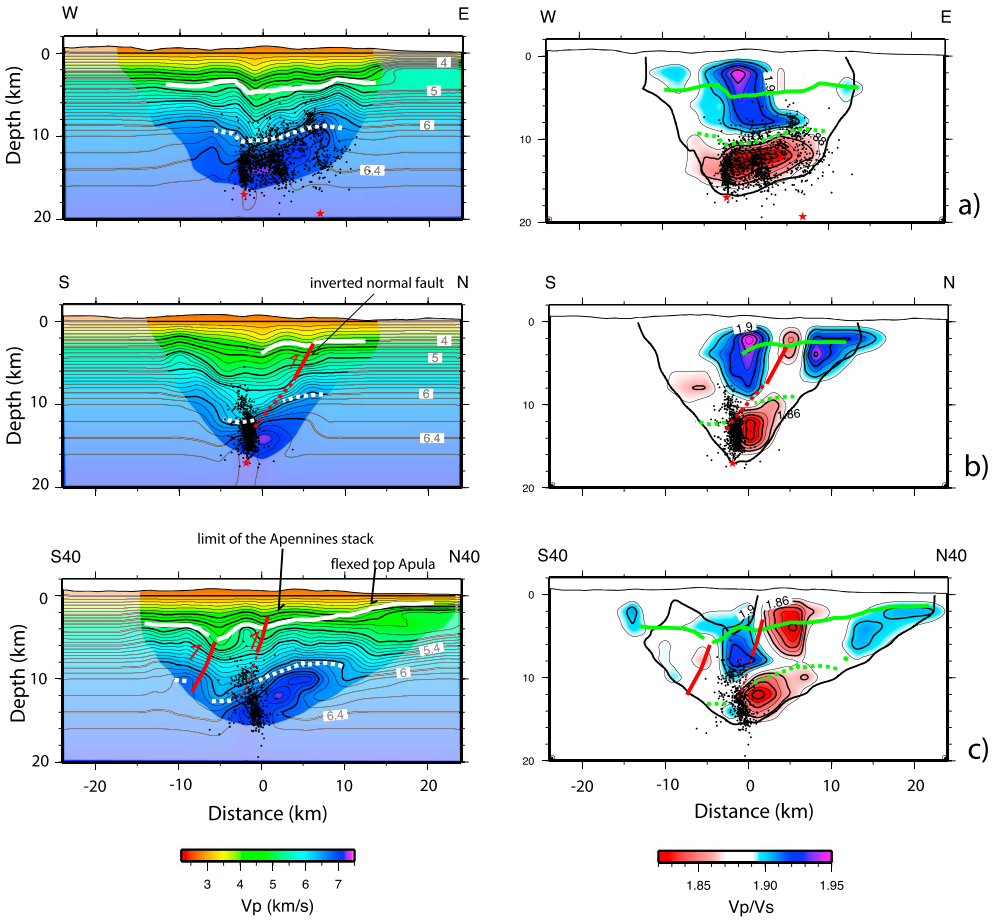

Figure 5. *Vp* and *Vp/Vs* models in three vertical sections cutting the 2002 ruptured fault. The white or green lines are the top (solid) or bottom (dashed) of the Apulian carbonate multilayer, from *Latorre et al.* [2010]. Red lines represent some major faults visible as warping of velocity anomalies. Aftershocks (black solid dots) and main shocks (red stars) occurring ±2.5 km from the sections are plotted.

4. Migration Images of Deep Crustal Seismic Reflections

Seismograms of the Molise sequence contain arrivals of secondary waves that we detected at almost all the stations of the network. In a previous work, we have investigated the seismic structure of the main crustal velocity contrast (the top of the Apulian carbonate) where the impacting seismic energy of the aftershocks generated high-amplitude *S-P* transmitted waves [*Latorre et al.,* 2010]. These waves are recorded between *P* and *S* first arrivals and show characteristic high frequencies and polarization on the vertical component.

A careful interpretation of the aftershock signals has evidenced the presence of another group of secondary waves that we have identified at some stations of the network. Unlike the converted waves at the Apulian platform top, these later phases are characterized by low frequencies and polarization on the horizontal components. The characteristics of their signal, together with their arrival times after the *S* wave, allow us to interpret these phases as either *P*-to-*S* or *S*-to-*S* reflections at a deep interface with strong impedance contrast.

In order to image the seismic discontinuity where these phases are generated, we analyze the signals of 120 well-located earthquakes recorded at ELI station. Our data choice is motivated by the high amplitude of the reflected signals recorded at this station and the location of the target volume, which is close to the area investigated by previous receiver function studies [*Bianchi*, 2010].

Figure 7 presents the waveforms of the selected earthquakes collected in seismic sections. In order to highlight the spatial coherence between signals, seismograms of vertical and radial components are shifted in time with respect to the *P* first arrival (zero time in the figure). Then, waveforms are sorted by considering

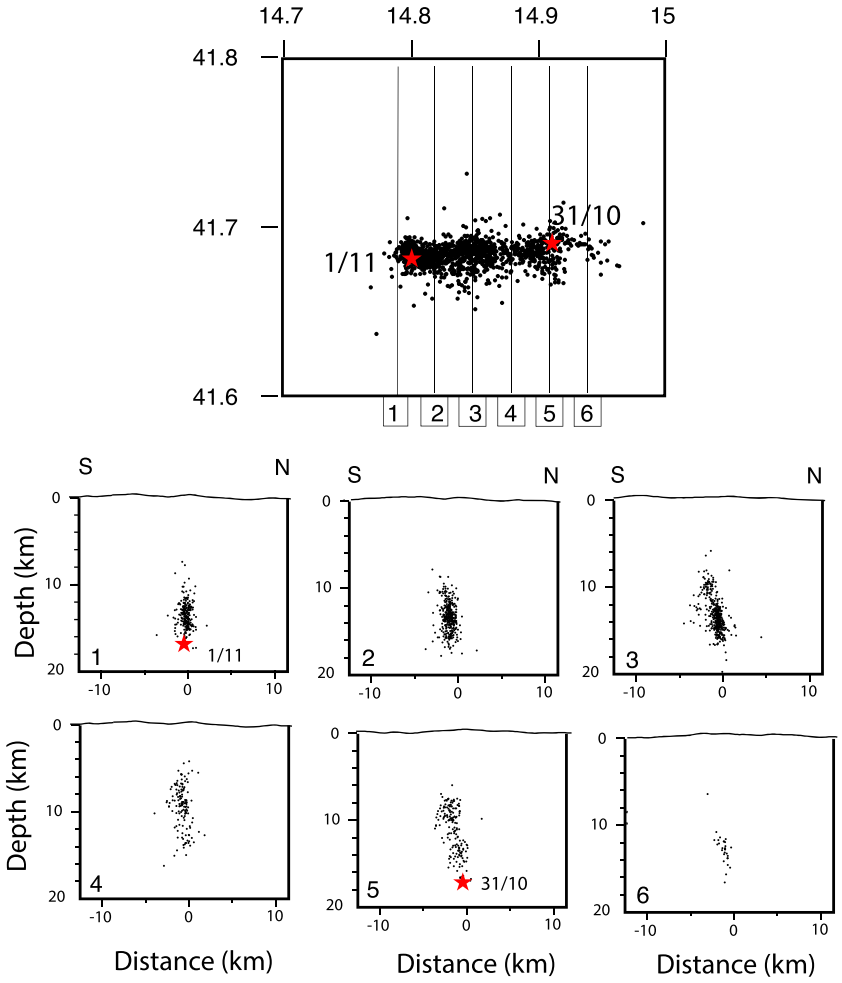

Figure 6. N-S trending vertical sections of main shocks (red stars, the date of occurrence is indicated) and 3-D-located aftershocks. Section traces are reported in the top panel.

the time difference between *S* and *P* first arrivals, which is indicative of source-to-receiver distance along the direct wave raypath. This kind of representation points out two main groups of secondary waves: the *S-P* transmitted waves at the Apulian platform top (green color in the figure) and the reflected waves analyzed in this study (red color). Reflected arrivals are well identified on the horizontal components between 1 and 2 s after the *S* wave arrival, while their energy is weaker on the vertical component.

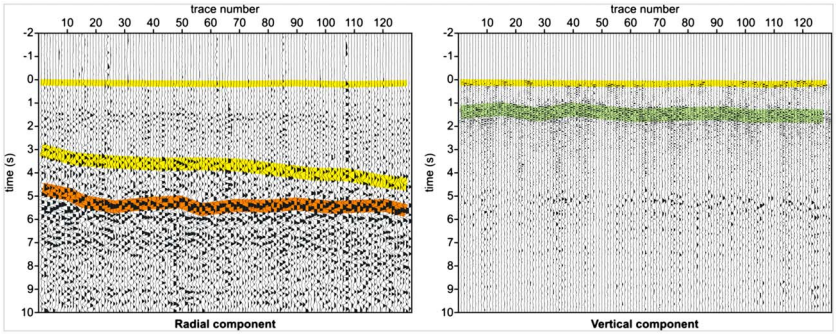

Figure 7. Seismic sections of radial and vertical component of waveforms recorded at ELI station. Traces are shifted with respect to the *P* first arrival time (zero time) and sorted by time difference between *S* and *P* first arrivals. Colors highlight the first arrivals of *P* and *S* waves (yellow), transmitted *S-P* waves at the top Apulian platform (green), and the reflected waves analyzed in this study (red).

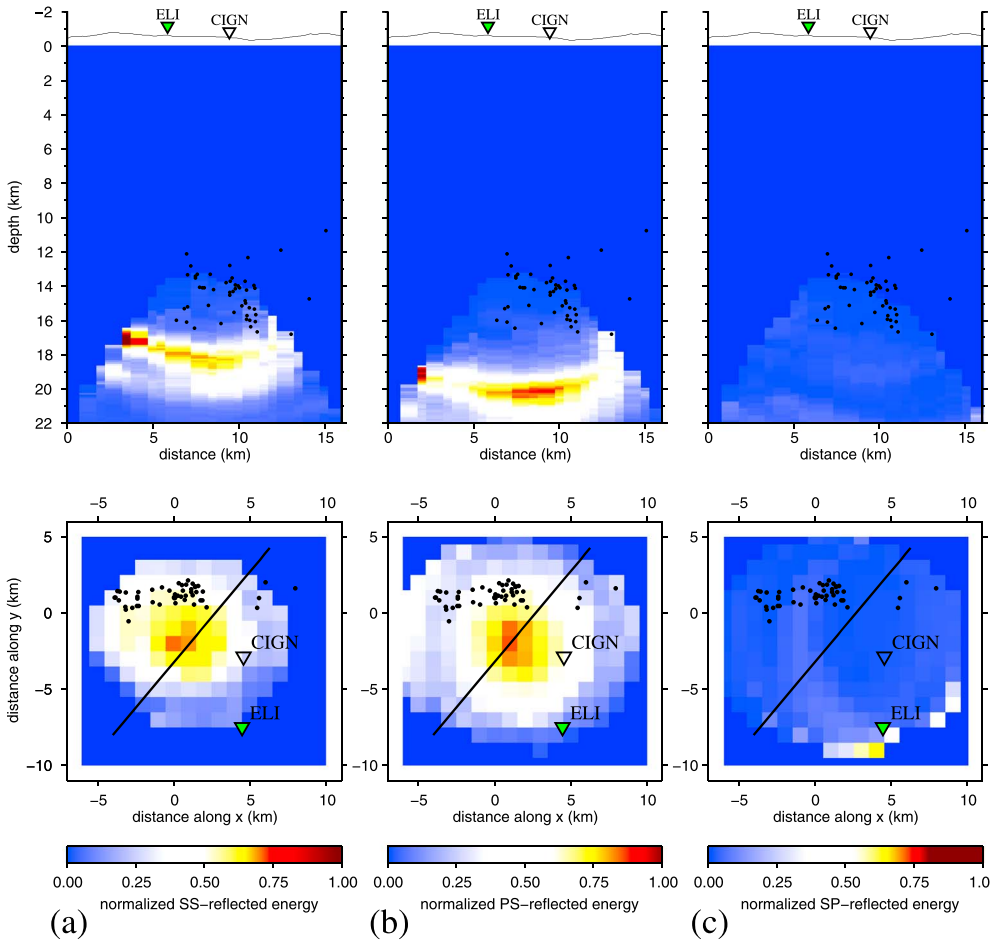

Figure 8. Vertical cross sections and map views of the migration models obtained by considering (a) *S-S* reflection mode, (b) *P-S* reflection mode, and (c) *S-P* reflection mode of propagation. Colors represent the amount of focused reflected energy at depth, normalized with respect to the maximum value of each model. Black dots indicate the earthquakes used in this analysis and recorded at the ELI station (green triangle). The black line indicates the trace of the cross section

Depth migration of the selected data set consisted in backprojecting the seismic signals in depth to image the crustal discontinuities where reflected waves can be generated. This is performed by applying the 3-D kinematic depth migration technique proposed by *Latorre et al.* [2008]. Seismic migration approaches with local earthquake data are useful to illuminate crustal structures at depths rarely reached by conventional studies of commercial seismic surveys [e.g., *Chavarria et al.*, 2003].

To migrate the seismic signals at depth, we divide the model volume with a grid of scattering points having horizontal distance of 500 m and vertical spacing of 100 m. We consider each earthquake as a shot, and we compute traveltimes of reflected waves from each source-receiver pair to each grid point of the model. Reflected traveltimes are computed in two steps through the three-dimensional tomographic model presented in this paper. First, we obtain wavefronts of first arrival times in a fine grid by using the finite difference code of *Podvin and Lecomte* [1991]. Then, we recalculate more accurate traveltimes after a posteriori ray tracing [see *Latorre et al.*, 2008 for further details].

For each grid point and source-receiver pair, the traveltime of the computed reflected wave identifies a segment of seismogram. Since we deal with different focal mechanisms and magnitudes, we only backproject in depth the square of the seismic amplitude recorded at the computed time. This amplitude is normalized and weighted using appropriate Snell's coefficients, and then it is associated to the grid point. The process is repeated for each source-receiver pair, and the seismic amplitudes from all the seismograms are stacked over the grid.

Data preprocessing consisted in (a) data filtering between 1 and 10 Hz, (b) three-component normalization of traces, and (c) muting of both *S* direct waves and the *S-P* transmitted waves at the Apulian platform (outlined with yellow and green colors in Figure 7, respectively).

After modeling, images reveal the zones at depth where migrated energies are focused, delineating the geometry of the seismic reflector. In Figure 8 we show two possible models of a deep crustal velocity contrast. Images are the result of two kinds of assumptions in the migration modeling by considering either an S-S reflection propagation mode (Figure 8a) or a P-S reflection propagation mode (Figure 8b). As comparison, we show the result of an S-P reflection mode migration, which does not indicate any particular focusing of seismic energy at depth (Figure 8c).

Both *P-S* and *S-S* migrated models image a strong reflector located close to the main shocks of the 2002 sequence. In the *S-S* model, the reflector appears shallower (about 18 km depth below the CIGN station) and seems to extend toward the southwest as a dipping interface. On the contrary, in the *P-S* model, the reflector is deeper (about 20 km depth below the CIGN station) and has a quite horizontal geometry.

From a kinematic point of view, both *S-S* and *P-S* reflection models are correct, since reflected seismic energies are well focused assuming both mode-converted wave propagations. On the contrary, other models, which assume different propagation modes (as *S-P* or *P-P* reflected waves), are not able to correctly explain the high-amplitude seismic waves presented in our data. Further elements to discriminate between *P-S* and *S-S* reflection models should come from careful analysis of amplitude variations. Unfortunately, up to now, migration techniques with passive sources do not take into account complex earthquake parameters such as magnitude, focal mechanisms, and directivity effects. On the other hand, both models are in agreement with the presence of a strong reflector at 18–20 km depth, which is reasonably compatible with a velocity reduction below the high speed *Vs* anomalies observed between 10 and 16 km depth in the tomographic model (Figure 5).

5. Discussion

The southern Apennines thrust and fold belt developed during the subduction and retreat of the Ionian slab from the accretion of Mesozoic sedimentary units on the Adria continental margin. Since about 0.7 Ma, an abrupt change of tectonics is documented for the southern Tyrrhenian system [*Westaway*, 1993] and referred to the development of a tear in the slab [*Rosenbaum and Lister*, 2004; *Chiarabba et al.*, 2008; *Ascione et al.*, 2012]. Accordingly, extensional deformation spread in the axial zone of the belt substituting compression [*Ascione et al.*, 2013, and references therein]. Present-day kinematic and GPS data suggest that compression is no longer active in the southern Apennines belt [*Devoti et al.*, 2011; *Montone et al.*, 2012], while the Eurasia-Nubia relative motion is accommodated by fragmentation of the Adriatic promontory and interaction between different sectors of Adria [*D'Agostino et al.*, 2008].

Despite the numerous studies on the formation and evolution of the belt and the relation with the southern Tyrrhenian subduction, the tectonic style of the Neogenic belt is still widely debated [*Butler et al.*, 2004; *Scrocca et al.*, 2005; *Mazzoli et al.,* 2008]. In thin-skinned models, the wedge is entirely made of Meso-Cenozoic sedimentary rocks stacked along a décollement at the Triassic evaporitic layer [*Bally et al.*, 1986; *Mostardini and Merlini*, 1986; *Scrocca et al.*, 2005; *Patacca et al.*, 2008]. Conversely, thick-skinned models imply that part of the metamorphic basement is incorporated in the wedge, resulting in a much smaller amount of shortening and subduction of the continental lithosphere [*Roure et al.*, 1991; *Tozer et al.*, 2002; *Butler et al.*, 2004]. Geophysical data are still not conclusive for supporting one of these two models, although they preferably support a thick-skinned model as explanation for the deep structure [*Improta and Corciulo*, 2006; *Speranza and Chiappini*, 2002; *Steckler et al.*, 2008].

The poor illumination in seismic lines below the sedimentary cover [*Mostardini and Merlini*, 1986; *Patacca and Scandone*, 1989; *Shiner et al.*, 2004] and the not-unique interpretation of midcrustal ultraspeed bodies [*Chiarabba and Amato,* 1997; *Bisio et al.*, 2004; *Improta and Corciulo*, 2006; *Chiarabba et al.*, 2010] make our understanding of the deep structure of the belt largely incomplete.

5.1. The Carbonate Multilayer and Tectonic Style

Our tomographic model shows the Apulian carbonate platform at depths between 4 and 10 km, consistent with deep seismic profiles [*Nicolai and Gambini*, 2007]. Velocity anomalies define the existence of a SW

dipping high-angle normal fault that cuts the carbonate platform (see sections b and c in Figure 5). The opposite warping of velocity contours in the deeper and shallower part of the fault suggests that the pristine normal fault is inverted, partially close to the leading edge, by subsequent inverse motion. Fault inversion with slip partitioning onto adjacent fault branches is very similar, but less developed, to that found in the Val d'Agri region of southern Apennines [see *Valoroso et al.*, 2011] that probably resulted from inversion of Permo-Triassic extensional basins [*Shiner et al.*, 2004]. In our case, we extend the inversion tectonics to forebulge/foredeep-related Pliocene normal faults with compression extending toward the external (eastern) area and influencing locally the geometry of the Apulian carbonate top, visible in seismic reconstructions [*Nicolai and Gambini*, 2007; *Latorre et al.*, 2010]. The velocity model clearly shows normal faults that developed during the flexure of the Apulian unit anticipating the belt advancement. As long as the leading edge of the belt propagated eastward, portions of the flexed lithosphere were involved in compression. The fault inversion documents a final stage of evolution of the belt, where compression is generalized to the entire, previously flexed, Apulian crust, consistent with the thick-skinned conclusive shortening proposed for the central southern Apennines [*Menardi Noguera and Rea*, 2000; *Shiner et al.*, 2004; *Mazzoli et al.*, 2008].

5.2. The High-Speed Bodies and the Pre-Mesozoic Basement

Very high *Vp* anomalies at midcrustal depth are observed (6.9 km/s, Figures 4 and 5), similarly to other regions of the Apennines. In this study, we document that the high-speed bodies are located beneath the Apulian sedimentary cover (Figure 5). In fact, the top of the Apulian platform is well constrained by tomographic velocity models, modeling of secondary arrivals [*Latorre et al.*, 2010], and independent data [*Nicolai and Gambini*, 2007], as well as the thickness of the sedimentary pile (see Puglia-1 well [*Patacca et al.*, 2008]). Our model shows a change of the *S* wave velocity within the basement across the E-W trending fault, consistent with the limit of strongly positive magnetic anomalies [see *Speranza and Chiappini*, 2002; *Caratori Tontini et al.*, 2004], suggesting a change in the rock type from a mafic, either intrusive or metamorphic (very high *Vp*, low *Vp*/*Vs*, very high susceptibility), to a more felsic basement (relatively high *Vp*, *Vp*/*Vs* values, low susceptibility). Our results indicate that the geometry of the high-velocity and positive magnetic bodies was already acquired before the final compressional phase of the Apennines. The broad distribution of such bodies in the middle crust of the Apennines [*Chiarabba et al.*, 2010] might suggest that parts of this complex basement made of high-speed, magnetic rocks are incorporated in the wedge, in agreement with the existence of a deep decoupling.

5.3. Middle Lower Crust Fluids and Deep Weakness Within Adria

We observe strong reflectivity at the base of the high-velocity body, consistent with the existence of a velocity inversion in the middle lower crust seen by regional tomography studies [see *Di Stefano et al.*, 2009]. A deep, strong reflectivity has been observed by the CROP11 seismic profile in the Adriatic external region [*Patacca et al.*, 2008]. This persistent layering may indicate a deep fluid-filled layer that potentially acts as a preferential weakness level for guiding deformation during continental delamination. The presence of such layering with a variable geometry and depth along the continental margin can account for the switch in time between thin- and thick-skinned tectonics, documented in the Apennines evolution. This deep fluid-filled layer probably acts as a main detachment for the deformation of the crust, today controlling the extent of extensional and transtensional faults in the brittle crust.

5.4. The Deep Structure and Inference on the 2002 Molise Earthquakes

Tectonic models that propose a primary role of an E-W trending, right-lateral strike-slip fault emerged after the 2002 earthquakes [*Di Bucci and Mazzoli*, 2003; *Di Bucci et al.*, 2006; *Boncio et al.*, 2007]. The fault system, which includes the Mattinata fault outcropping in the Gargano area, is elongated for about 180 km from the Adriatic offshore to the mountain belt [*Billi et al.*, 2007]. The occurrence of large historical earthquakes on this structure, such as the 1627 *M* 6.7 event, is discussed and controversial [*Patacca and Scandone*, 2004; *Rovida et al.*, 2011]. More recently, GPS velocities showed that the prevailing deformation is the extension along the mountain belt [*D'Agostino et al.*, 2008; *Devoti et al.*, 2011], while preexisting faults of the Apulian margin accommodate differential deformation within the continental Adria microplate. Considering the lack of consensus on the role played by the E-W fault in the today tectonics [see *Argnani et al.*, 2009], we restrict our focus on two new aspects that are inherent to our results.

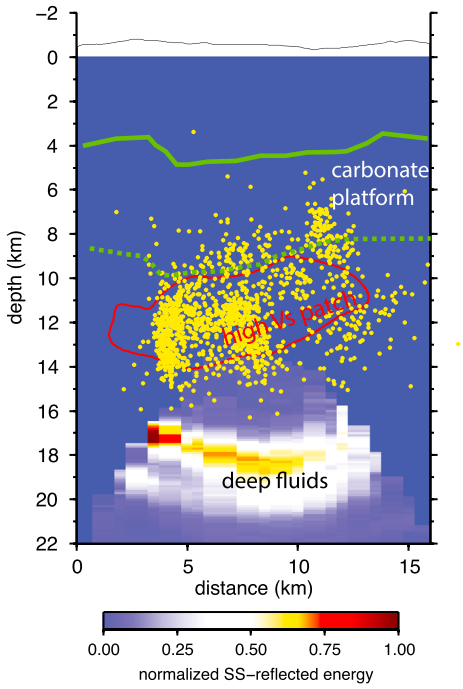

Figure 9. Sketch of the 2002 ruptured fault. The green lines indicate the top and bottom of the Apulia carbonate platform. The encircled area is the high *Vp*, low *Vp*/*Vs*, very high *Vs* patch in the Adria basement. Note that the two main shocks originated close to this deep layer and the aftershocks concentrated within the high *Vs* patch in the basement.

First, the 2002 earthquake sequence developed predominantly within the Apulian basement (Figure 5). A few earthquakes occurred in the carbonate multilayer, only in a small area of the eastern portion of the fault system, where also the main shock rupture top depth was shallower [*Vallée and Di Luccio*, 2005]. The absence of seismicity in the carbonate multilayer is not easy to explain, since this layer is indeed brittle and generally ruptured during moderate to large magnitude earthquakes of the Apennines [*Amato et al.*, 1992; *Di Stefano et al.*, 2009]. The unusual depth of seismicity is also consistent with the predominant depth of background seismicity in the Gargano area [see *Chiarabba et al.*, 2005]. Second, the activated portion of the fault corresponds to a transition of body waves velocities (Figure 4), presumably a lateral heterogeneity of the basement acquired during the previous activity of the fault system. Together, these two lines of evidence suggest that the deep sharp velocity contrast represents a weakness zone along which moderate to slightly large magnitude earthquakes can be triggered in this area of relatively small deformation close to the foreland of the southern Apennines. The slow rupture velocity observed for this earthquake and the reduced capability to trigger dynamically the rupture on adjacent segments [*Vallée and Di Luccio*, 2005] are consistent with the hypothesis that localized deep patches in the basement are probably weak. The presence of sharp reflectivity at the depth of the main shocks hypocenters (see Figure 9) supports the hypothesis that deep fluids may favor the unlocking of weak patches along preexisting discontinuities of the basement. This process is probably related to differential deformation within the Adria lithosphere.

6. Conclusion

In this study, we provide new original information that help understanding the structure and tectonics of southern Apennines.

The structure of the crust consists of a 6 km thick relatively high *Vp*, high *Vp*/*Vs* carbonate multilayer underlaying a relatively thin low *Vp* cover that is thicker moving westward. These sedimentary units overlay a 6–8 km thick high *Vp*, high to low *Vs* pre-Alpine heterogeneous basement that is bottomed by a layer with strong reflectivity at about 20 km depth. Three main features are revealed by tomography and reflected wave depth migration: (i) inverted normal faults within the Apulian sedimentary cover, (ii) exceptionally high-speed bodies beneath the sedimentary cover, and (iii) strong reflectivity in the middle lower crust.

1. Velocity anomalies document a west dipping normal fault developed in the sedimentary cover, due to the flexure of the Adria lithosphere before the compression. The warping of velocity anomalies shows that the normal fault is inverted. Fault inversion, which is incomplete close to the leading edge of the Apennines compressional belt, is consistent with a thick-skinned final episode in the southern Apennines formation.
2. To understand the Apennines tectonics, one key element is the nature of high-velocity bodies broadly observed in the midcrust beneath the belt. In this study we show that the high-velocity rocks are located beneath the sedimentary cover and represent heterogeneities of the pre-Alpine basement. The observation of similar bodies under the mountain range suggests that they are accreted in the belt together with the sedimentary cover.

3. The presence of diffuse reflectivity suggests fluid-filled layering in the middle lower crust. The today active strike-slip tectonics is favored by deep fluids, which trigger ruptures on spot-like, weak patch of the Apulia basement. At a regional scale, the seismicity diffused in the Apulian region at middle-to-lower crustal depth [see *Chiarabba et al.*, 2005] may be favored by the existence of these hydrated layers in the lower crust.

Our results have an impact in explaining the evolution of the southern Apennines belt and potentially of other continental collision zones. The reconnaissance of the Adria pristine structure permits some speculation on the general evolution of the Apennines. The existence of fossilized fluids compartments in the middle lower crust may be the primary weakness level that localizes the deformation of the lithosphere during the continental collision, favoring the décollement of shallow units accreted to the belt from the delaminated lithosphere.

Acknowledgments
We thank Onno Oncken, Claudio Faccenna, Ulrich Achauer, and two anonymous reviewers for helpful comments. The data for this paper, arrival times data, station coordinates, and earthquake locations are free and available upon request at claudio.chiarabba@ingv.it.

References

Amato, A., C. Chiarabba, L. Malagnini, and G. Selvaggi (1992), Three-dimensional *P*-velocity structure in the region of the *Ms* 6.9 Irpinia, Italy, normal faulting earthquake, *Phys. Earth Planet. Inter.*, *75*, 111–119.

Argnani, A., M. Rovere, and C. Bonazzi (2009), Tectonics of the Mattinata fault, offshore south Gargano (southern Adriatic Sea, Italy): Implications for active deformation and seismotectonics in the foreland of the Southern Apennines, *GSA Bull.*, *121*(9-10), 1421–1440, doi:10.1130/B26326.1.

Ascione, A., S. Ciarcia, V. Di Donato, S. Mazzoli, and S. Vitale (2012), The Pliocene-Quaternary wedge-top basins of southern Italy: An expression of propagating lateral slab tear beneath the Apennines, *Basin Res.*, *24*, 456–474, doi:10.1111/j.1365-2117.2011.00534.x.

Ascione, A., S. Mazzoli, P. Petrosino, and E. Valente (2013), A decoupled kinematic model for active normal faults: Insights from the 1980, *MS* = 6.9 Irpinia earthquake, southern Italy, *Geol. Soc. Am. Bull.*, *125*, 1239–1259, doi:10.1130/B30814.1.

Bally, A. W., L. Burbi, C. Cooper, and R. Ghelardoni (1986), Balanced sections and seismic reflection profiles across the central Apennines, *Mem. Soc. Geol. It.*, *35*, 257–310.

Bianchi, I. (2010), Velocity structure and seismic anisotropy in the crust and upper mantle from receiver function analysis: Three case studies in Italy, PhD thesis, Bologna 2010.

Billi, A., R. Gambini, C. Nicolai, and F. Storti (2007), Neogene-Quaternary intraforeland transpression along a Mesozoic platform-basin margin: The Gargano fault system, Adria, Italy, *Geosphere*, *3*, 1–15, doi:10.1130/GES00057.1.

Bisio, L., R. Di Giovanbattista, G. Milano, and C. Chiarabba (2004), Three-dimensional earthquake locations and upper crustal structure of the Sannio-Matese region (southern Italy), *Tectonophysics*, *385*, 121–136, doi:10.1016/j.tecto.2004.01.007.

Boncio, P., T. Mancini, G. Lavecchia, and G. Selvaggi (2007), Seismotectonics of strike-slip earthquakes within the deep crust of southern Italy: Geometry, kinematics, stress field and crustal rheology of the Potenza 1990–1991 seismic sequences (Mmax5.7), *Tectonophysics*, *445*, 281–300, doi:10.1016/j.tecto.2007.08.016.

Butler, R. W. H., et al. (2004), Applying thick-skinned tectonic model to the Apennine thrust-belt of Italy: Limitations and implications, in *Thrust Tectonic and Hydrocarbon System, Am. Assoc. of Pet. Geol. Mem.*, vol. 82, edited by K. R. McClay, pp. 647–667.

Butler, R. W. H., E. Tavarnelli, and M. Grasso (2006), Structural inheritance in mountain belts: An Alpine-Apennine perspective, *J. Struct. Geol.*, *28*, 1893–1908.

Caratori Tontini, F., P. Stefanelli, I. Giori, O. Faggioni, and C. Carmisciano (2004), The revised aeromagnetic anomaly map of Italy, *Ann. Geophys.*, *47*, 5.

Chavarria, J. A., P. E. Malin, R. D. Catchings, and E. Shalev (2003), A look inside the San Andreas Fault at Parkfield through vertical seismic profiling, *Science*, *302*, 1746–1748, doi:10.1126/science.1090711.

Chiarabba, C., and A. Amato (1997), Upper-crustal structure of the Benevento area (southern Italy): Fault heterogeneities and potential for large earthquakes, *Geophys. J. Int.*, *130*, 229–239, doi:10.1111/j.1365-246X.1997.tb01001.x.

Chiarabba, C., and A. Amato (2003), Vp and Vp/Vs images in the *Mw* 6.0 Colfiorito fault region (central Italy): A contribution to the understanding of seismotectonic and seismogenic processes, *J. Geophys. Res.*, *108*(B5), 2248, doi:10.1029/2001JB001665.

Chiarabba, C., et al. (2005), Main shocks and aftershocks of the 2002 Molise seismic sequence, southern Italy, *J. Seismol.*, *9*(4), 487–494, doi:10.1007/s10950-005-0633-9.

Chiarabba, C., P. De Gori, and F. Speranza (2008), The southern Tyrrhenian subduction zone: Deep geometry, magmatism and Plio-Pleistocene evolution, *Earth Planet. Sci. Lett.*, *268*, 408–423.

Chiarabba, C., P. De Gori, and F. Speranza (2009), Deep geometry and rheology of an orogenic wedge developing above a continental subduction zone: Seismological evidence from the northern-central Apennines (Italy), *Lithosphere*, *1*, 95–104, doi:10.1130/L34.1.

Chiarabba, C., S. Bagh, I. Bianchi, P. De Gori, and M. Barchi (2010), Deep structural heterogeneities and the tectonic evolution of the Abruzzi region (central Apennines, Italy) revealed by microseismicity, seismic tomography and teleseismic receiver functions, *Earth Planet. Sci. Lett.*, *295*, 462–476.

D'Agostino, N., A. Avallone, D. Cheloni, E. D'Anastasio, S. Mantenuto, and G. Selvaggi (2008), Active tectonics of the Adriatic region from GPS and earthquake slip vectors, *J. Geophys. Res.*, *113*, B12413, doi:10.1029/2008JB005860.

Dercourt, J., et al. (1986), Geological evolution of the Tethys belt from the Atlantic to the Pamirs since the LIAS, *Tectonophysics*, *123*, 241–315, doi:10.1016/0040-1951(86)90199-X.

Devoti, R., A. Esposito, G. Pietrantonio, A. R. Pisani, and F. Riguzzi (2011), Evidence of large scale deformation patterns from GPS data in the Italian subduction boundary, *Earth Planet. Sci. Lett.*, *311*, 230–241, doi:10.1016/j.epsl.2011.09.034.

Dewey, J. F., M. L. Helman, E. Turco, D. H. W. Hutton, and S. D. Knott (1989), Kinematics of the western Mediterranean, in *Alpine Tectonics*, *Spec. Publ. Geol. Soc.*, vol. 45, 265–283, Geological Society of London, London.

Di Bucci, D., and S. Mazzoli (2003), The October-November 2002 Molise seismic sequence (southern Italy): An expression of Adria intraplate deformation, *J. Geol. Soc.*, *160*(4), 503–506, doi:10.1144/0016-764902-152.

Di Bucci, D., A. Ravaglia, S. Seno, G. Toscani, U. Fracassi, and G. Valensise (2006), Seismotectonics of the southern Apennines and Adriatic foreland: Insights on active regional E-W shear zones from analogue modeling, *Tectonics*, *25*, TC4015, doi:10.1029/2005TC001898.

Di Luccio, F., E. Fukuyama, and N. A. Pino (2005), The 2002 Molise earthquake sequence: What can we learn about the tectonics of southern Italy?, Tectonophysics, *405*, 141–154, doi:10.1016/j.tecto.2005.05.024.

Di Stefano, R., E. Kissling, C. Chiarabba, A. Amato, and D. Giardini (2009), Shallow subduction beneath Italy: Three-dimensional images of the Adriatic-European-Tyrrhenian lithosphere system based on high-quality *P* wave arrival times, *J. Geophys. Res.*, *114*, B05305, doi:10.1029/2008JB005641.

Doglioni, C., P. Harabaglia, G. Martinelli, F. Mongelli, and G. Zito (1996), A geodynamic model of the southern Apennines accretionary prism, *Terra Nova*, *8*, 540–547.

Giacomuzzi, G., C. Chiarabba, and P. De Gori (2010), Linking the Alps and Apennines subduction systems: New constraints revealed by high-resolution teleseismic tomography, *Earth Planet. Sci. Lett.*, *301*, 531–543, doi:10.1016/j.epsl.2010.11.033.

Haslinger, F. (1998) Velocity structure, seismicity and seismotectonics of northwestern Greece between the Gulf of Arta and Zakynthos, PhD thesis, Dep. Geophys., ETH, Zurich, Switzerland.

Improta, L., and M. Corciulo (2006), Controlled source non linear tomography: A powerful tool to constrain tectonic models of the Southern Apennines orogenic wedge, Italy, *Geology*, *34*(11), 941–944, doi:10.1130/G22676A.1.

Jolivet, L., and C. Faccenna (2000), Mediterranean extension and the African-Eurasian collision, *Tectonics*, *19*, 1095–1106.

Jolivet, L., C. Faccenna, and C. Piromallo (2009), From mantle to crust: Stretching the Mediterranean, *Earth Planet. Sci. Lett.*, *285*, 198–209, doi:10.1016/j.epsl.2009.06.017.

Latorre, D., P. De Gori, C. Chiarabba, A. Amato, J. Virieux, and T. Monfret (2008), Three dimensional kinematic depth migration of converted waves: Application to the 2002 Molise aftershock sequence (southern Italy), *Geophys. Prospect.*, *56*, 587–600, doi:10.1111/j.1365-2478.2008.00711.x.

Latorre, D., A. Amato, and C. Chiarabba (2010), High-resolution seismic imaging of the *Mw*5.7, 2002 Molise, southern Italy, earthquake area: Evidence of deep fault reactivation, *Tectonics, 29*, TC4014, doi:10.1029/2009TC002595.

Lister, G. S., M. A. Etheridge, and P. A. Symonds (1986), Detachment faulting and the evolution of passive continental margins, *Geology*, *14*, 246–250, doi:10.1130/0091-7613(1986)14.

Lucente, P., C. Chiarabba, G. B. Cimini, and D. Giardini (1999), Tomographic constraints on the geodynamical evolution of the Italian region, *J. Geophys. Res.*, *104*, 20,307–20,327.

Mariotti, G., and C. Doglioni (2000), The dip of the foreland monocline in the Alps and Apennines, *Earth Planet. Sci. Lett.*, *181*, 191–202, doi:10.1016/S0012-821X(00)00192-8.

Mazzoli, M., M. D'Errico, L. Aldega, S. Corrado, C. Invernizzi, P. Shiner, and M. Zattin (2008), Tectonic burial and "young" (<10 Ma) exhumation in the southern Apennines fold-and-thrust belt (Italy), *Geology*, *36*, 243–246, doi:10.1130/G24344A.1.

Mazzoli, S., L. Aldega, S. Corrado, C. Invernizzi, and M. Zattin (2006), Pliocene-Quaternary thrusting, synorogenic extension and tectonic exhumation in the southern Apennines (Italy): Insights from the Monte Alpi area, in *Styles of Continental Contraction*, edited by S. Mazzoli and R. W. H. Butler, *Spec. Pap. Geol. Soc. Am.*, *414*, 55–77, doi:10.1130/2006.2414(04).

Menardi Noguera, A., and G. Rea (2000), Deep structure of the Campanian-Lucanian Arc (southern Apennine, Italy), *Tectonophysics*, *324*, 239–265, doi:10.1016/S0040-1951(00)00137-2.

Menke, W. (1989), *Geophysical Data Analysis: Discrete Inverse Theory*, *Int. Geophys. Ser.*, vol. 45, 285 pp., Academic, San Diego, Calif.

Michelini, A., and T. V. McEvilly (1991), Seismological studies at Parkfield, I, simultaneous inversion for velocity structure and hypocentres using cubic b-splines parameterization, *Bull. Seismol. Soc. Am.*, *81*, 524–552.

Montone, P., M. T. Mariucci, and S. Pierdominici (2012), The Italian present-day stress map, *Geophys. J. Int.*, *189*, 705–716, doi:10.1111/j.1365-246X.2012.05391.x.

Mostardini, F., and S. Merlini (1986), Appennino centro-meridionale. Sezioni Geologiche e Proposta di Modello Strutturale, *Mem. Soc. Geol. Ital.*, *35*, 177–202.

Nicolai, C., and R. Gambini (2007), Structural architecture of the Adria platform-and-basin system, *Boll. Soc. Geol. Ital.*, *7*, 21–37.

Patacca, E., and P. Scandone (1989), Post-Tortonian mountain building in the Apennines: The role of the passive sinking of a relic lithospheric slab, in *The Lithosphere in Italy: Advances in Earth Science Research*, Atti Conv. Lincei, vol. 80, edited by A. Boriani et al., pp. 157–176, Rome.

Patacca, E., and P. Scandone (2004), The 1627 Gargano earthquake (southern Italy): Identification and characterization of the causative fault, *J. Seismol.*, *8*, 259–273, doi:10.1023/B:JOSE.0000021393.77543.1e.

Patacca, E., and P. Scandone (2007), Geological interpretation of the CROP04 seismic line (southern Apennines, Italy), *Boll. Soc. Geol. Ital.*, *7*, 297–315.

Patacca, E., P. Scandone, E. Di Luzio, G. P. Cavinato, and M. Parotto (2008), Structural architecture of the central Apennines: Interpretation of the CROP 11 seismic profile from the Adriatic coast to the orographic divide, *Tectonics*, *27*, TC3006, doi:10.1029/2005TC001917.

Piromallo, C., and A. Morelli (2003), P wave tomography of the mantle under the Alpine–Mediterranean area. *J. Geophys. Res. 108*(B2), 2065, doi:10.1029/2002JB001757.

Podvin, P., and I. Lecomte (1991), Finite difference computation of travel time in very contrasted velocity model: A massively parallel approach and its associated tools, *Geophys. J. Int.*, *105*, 271–284, doi:10.1111/j.1365-246X.1991.tb03461.x.

Rosenbaum, G., and G. S. Lister (2004), Neogene and Quaternary rollback evolution of the Tyrrhenian Sea, the Apennines, and the Sicilian Maghrebides, *Tectonics*, *23*, TC1013, doi:10.1029/2003TC001518.

Roure, F., P. Casero, and R. Vially (1991), Growth process and melange formation in the southern Apennines accretionary wedge, *Earth Planet. Sci. Lett.*, *102*, 395–412, doi:10.1016/0012-821X(91)90031-C.

A. Rovida, R. Camassi, P. Gasperini and M. Stucchi (Eds.) 2011. CPTI11, The 2011 version of the parametric catalogue of Italian earthquakes, Milano, Bologna, doi:10.6092/INGV.IT-CPTI11. [Available at http://emidius.mi.ingv.it/CPTI.]

Royden, L. E., E. Patacca, and P. Scandone (1987), Segmentation and configuration of subducted lithosphere in Italy: An important control on thrust-belt and foredeep-basin evolution, *Geology*, *15*, 714–717.

Scrocca, D., E. Carminati, and C. Doglioni (2005), Deep structure of the southern Apennines, Italy: Thin-skinned or thick-skinned?, *Tectonics*, *24*, TC3005, doi:10.1029/2004TC001634.

Shiner, P., A. Beccaccini, and S. Mazzoli (2004), Thin-skinned versus thick-skinned structural models for Apulian carbonate reservoirs: Constraints from the Val d'Agri Fields, S. Apennines, Italy, *Mar. Pet. Geol.*, *21*, 805–827, doi:10.1016/j.marpetgeo.2003.11.020.

Speranza, F., and M. Chiappini (2002), Thick-skinned tectonics in the external Apennines, Italy: New evidence from magnetic anomaly analysis, *J. Geophys. Res.*, *107*, 2290, doi:10.1029/2000JB000027.

Steckler, M. S., N. PianaAgostinetti, C. K. Wilson, P. Roselli, L. Seeber, A. Amato, and A. L. Lam (2008), Crustal structure in the southern Apennines from teleseismic receiver functions, *Geology*, *36*(2), 155–158.

Tavani, S., A. Iannace, S. Mazzoli, S. Vitale, and M. Parente (2013), Late Cretaceous extensional tectonics in Adria: Insights from soft-sediment deformation in the Sorrento peninsula (southern Apennines), *J. Geodyn.*, *68*, 49–59, doi:10.1016/j.jog.2013.03.005.

Thurber, C. H. (1983), Earthquake locations and three-dimensional crustal structure in the Coyote Lake area, central California, *J. Geophys. Res.*, *88*(B10), 8226–8236, doi:10.1029/JB088iB10p08226.

Toomey, D. R., and G. R. Foulger (1989), Tomographic inversion of local earthquakes data from the Hengill-Grendsalur Central Volcano Complex, Iceland, *J. Geophys. Res.*, *94*, 17,497–17,510.

Tozer, R. S. J., R. W. H. Butler, and S. Corrado (2002), Comparing thin- and thick-skinned tectonic models of the central Apennines, Italy, in *Continental Collision and the Tectono-Sedimentary Evolution of Forelands*, *Stephan Mueller Spec. Publ. Ser.*, vol. 1, edited by G. Bertotti, K. Schulmann, and S. A. P. L. Cloetingh, pp. 181–194, Eur. Geophys. Union.

Um, J., and C. H. Thurber (1987), A fast algorithm for two-point seismic ray tracing, *Bull. Seismol. Soc. Am.*, *77*, 972–986.

Vallée, M., and F. Di Luccio (2005), Source analysis of the 2002 Molise (southern Italy) twin earthquakes (10/31 and 11/01), *Geophys. Res. Lett.*, *32*, L12309, doi:10.1029/2005GL022687.

Valoroso, L., L. Improta, P. De Gori, and C. Chiarabba (2011), Upper crustal structure, seismicity and pore pressure variations in an extensional seismic belt through 3D and 4D Vp and Vp/Vs models: The example of the Val d'Agri area (southern Italy), *J. Geophys. Res.*, *116*, B07303, doi:10.1029/2010JB007661.

Vitale, S., F. Dati, S. Mazzoli, S. Ciarcia, V. Guerriero, and A. Iannace (2012), Modes and timing of fracture network development in poly-deformed carbonate reservoir analogues, Mt. Chianello, southern Italy, *J. Struct. Geol.*, *37*, 223–235, doi:10.1016/j.jsg.2012.01.005.

Westaway, R. (1993), Quaternary uplift of southern Italy, *J. Geophys. Res.*, *98*, 21,741–21,772.